

# Deep learning pipeline reveals key moments in human embryonic development predictive of live birth after in vitro fertilization

Camilla Mapstone<sup>1,2</sup>, Helen Hunter<sup>3</sup>, Daniel Brison <sup>3,4</sup>, Julia Handl<sup>2</sup> Berenika Plusa <sup>1,\*</sup>

<sup>1</sup>Faculty of Biology, Medicine and Health (FBMH), Division of Developmental Biology & Medicine, University of Manchester, Manchester, M13 9PT, United Kingdom

<sup>2</sup>Alliance Manchester Business School, University of Manchester, Manchester, M15 6PB, United Kingdom

<sup>3</sup>Department of Reproductive Medicine, Old Saint Mary's Hospital, Manchester University NHS Foundation Trust, Manchester Academic Health Science Centre, Manchester, M13 0JH, United Kingdom

<sup>4</sup>Division of Developmental Biology and Medicine, Maternal and Fetal Health Research Centre, School of Medical Sciences, Faculty of Biology Medicine and Health, University of Manchester, Manchester Academic Health Science Centre, Manchester, M13 9WL, United Kingdom

\*Correspondence address. Faculty of Biology, Medicine and Health (FBMH), Division of Developmental Biology & Medicine, University of Manchester, Michael Smith Building, Manchester, M13 9PT, United Kingdom. Tel: +44 16127 51563; fax:+44 (0) 1612751491. E-mail: Berenika.Plusa@manchester.ac.uk

## Abstract

Demand for in vitro fertilization (IVF) treatment is growing; however, success rates remain low partly due to difficulty in selecting the best embryo to be transferred. Current manual assessments are subjective and may not take advantage of the most informative moments in embryo development. Here, we apply convolutional neural networks (CNNs) to identify key windows in pre-implantation human development that can be linked to embryo viability and are therefore suitable for the early grading of IVF embryos. We show how machine learning models trained at these developmental time points can be used to refine overall embryo viability assessment. Exploiting the well-known capabilities of transfer learning, we illustrate the performance of CNN models for very limited datasets, paving the way for the use on a clinic-by-clinic basis, catering for local data heterogeneity.

**Keywords:** IVF, human embryo assessment, blastocyst, Machine learning

## Introduction

Machine learning (ML) has already demonstrated great promise in many areas of medical imaging [1–3] and has the potential to revolutionize the field of medical diagnostics. There has been recent interest in applying ML approaches to tackle infertility, a growing health crisis impacting both individuals and society that has led to a rising demand for in vitro fertilization (IVF) treatments [4]. Due to low success rates, multiple IVF attempts are often required, leading to additional costs and distress for the patients. One of the main challenges in IVF is the difficulty in selecting an embryo to be transferred, as the general consensus on what the healthy, human embryo looks like, and which embryos are the most suitable for transfer is still under extensive debate [5–7]. The selection process routine in most clinics involves visual assessment of embryos in real-time or via time-lapse videos. Embryos are assessed based on morphological features such as the number and size of cells at the cleavage stage and in the trophectoderm (TE) and inner cell mass (ICM) in the blastocyst (Fig. 1A), the expansion of the cavity, developmental timings, cellular fragmentation, and multi-nucleation. This manual assessment is subjective, with up to 83% variation between embryologists [8], and uses only a fraction of the information that is potentially available. A convolutional neural network (CNN)-based approach that automatically assesses embryos

using more extensive information from across the time-lapse videos could potentially provide a consistent and reproducible method for embryo selection [9].

In recent years, many CNN approaches to assessing embryo viability have been developed [8, 10–23], demonstrating the potential for deep learning to inform embryo selection. Most of these CNN-based studies focus on the blastocyst stage, mirroring the most widely used process of embryo selection by trained embryologists. Although embryologists may pay attention to earlier stages, there is no consensus on which stages are crucial to look at and there is no standardized method of combining morphological features and/or assigned grades from across development into a single overall viability score. A few CNN-based approaches have incorporated frames from earlier embryonic stages [12, 15, 17, 22, 23], and some have succeeded in making viability assessments using solely pre-blastocyst stages [15, 17, 23], demonstrating that it is possible for CNNs to extract information about embryo viability from this early developmental period. It is yet to be determined whether there are specific moments in this period that are particularly informative, and therefore, the choice of which frames to include requires further investigation. This choice could impact model performance, as frame selection based just on video timestamp could miss crucial moments or add unnecessary data, potentially leading to overfitting. Identifying

Received: 21 May 2024. Revised: 12 July 2024. Editorial decision: 15 July 2024. Accepted: 18 July 2024

© The Author(s) 2024. Published by Oxford University Press.

This is an Open Access article distributed under the terms of the Creative Commons Attribution-NonCommercial License (<https://creativecommons.org/licenses/by-nc/4.0/>), which permits non-commercial re-use, distribution, and reproduction in any medium, provided the original work is properly cited. For commercial re-use, please contact journals.permissions@oup.com

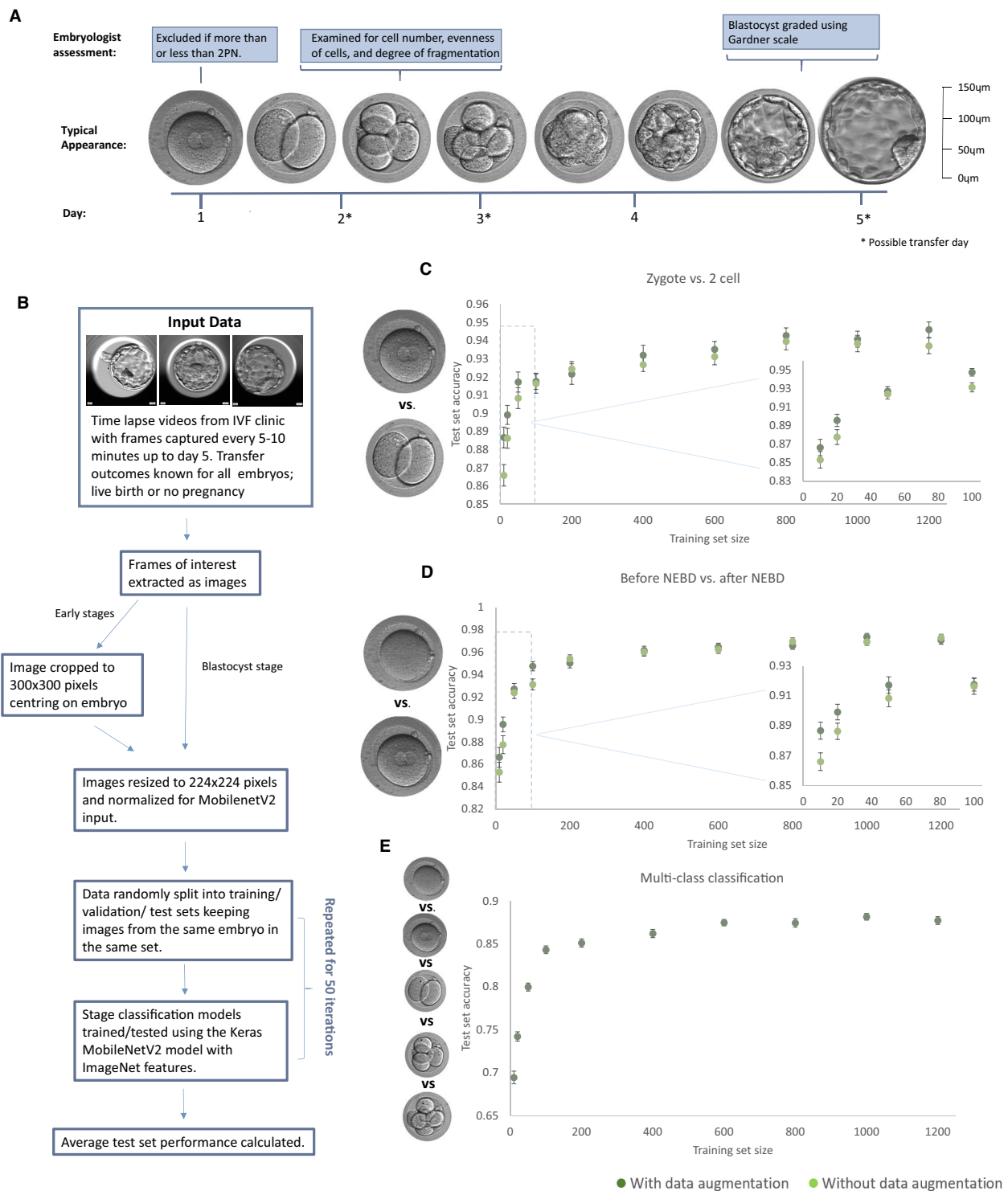


**Figure 1.** Performance of developmental stage classification models with increasing amount of training data. **(A)** The typical development of human embryo and an overview of embryologist assessments carried out at each stage. **(B)** The methodology of training developmental stage classification models from time-lapse data. **(C)** The accuracy of the test set on models trained to classify an image as zygote or 2-cell with varying amounts of training data. **(D)** The accuracy of the test set on models trained to classify an image as before NEBD or after NEBD with varying amounts of training data. **(E)** The accuracy of the test set on multi-class models trained to classify an image into one out of five developmental stage classes with varying amounts of training data. Subparts **(C–E)** show the average scores over 50 training attempts with 25 embryos in each class for the test and validation set. The accompanying error bars are the standard error across these 50 training attempts.

moments in development that are most predictive of live birth could lead towards further improvements in viability assessment, based on the most important information across development.

In this work, we used a CNN to determine the moments in development that can be linked to higher embryo viability (defined

as the most predictive of live birth) and demonstrated the importance of including these developmental time-points when assessing embryo viability. First, through the development of a stage classification algorithm, we demonstrated the high efficiency of our chosen model in correctly classifying stages of

pre-implantation embryos. We then showed that this ML framework can assess blastocyst viability at a similar level to embryologists. Subsequently, we successfully applied this model to predict live births at earlier stages, for which no standardized assessment methods exist. Capitalizing on that, we used ML to identify previously unknown pivotal time-points for live birth prediction in the pre-blastocyst embryo, which is a first step for better understanding of the biology of human development and offers the means for better overall viability assessment and/or earlier transfer. Finally, we showed that combining information from our identified time-points of embryo development with blastocyst stage predictions allows for a quantitative ranking of high-quality blastocysts that could not have been achieved by any of the existing assessment methods. Critical to widespread clinical application, our findings also confirm that it is possible to train a CNN model in this domain to a high standard using limited data.

## Material and methods

### Patients and time-lapse videos

Time-lapse videos of developing embryos were supplied by the IVF clinic in the Department of Reproductive Medicine at Old Saint Mary's Hospital, Manchester University NHS Foundation Trust, Manchester, UK. Embryos were cultured in either the Embryoscope™ or Embryoscope+™ time-lapse incubator system (Vitrolife, Sweden). Throughout the study period, there were no changes to the culture media or other culture conditions. Embryos were cultured in GTL overlaid with Ovoil (Vitrolife, Sweden) from post-injection (after ICSI, approximately 40 h post-human chorionic gonadotropin (hCG) trigger) to day 5 of development. Embryoscope™ slides can hold up to 12 embryos in individual wells with 25 µl of media, overlaid with 1.2 ml of oil. Embryoscope+™ slides can hold up to 16 embryos, in 2 rows of 8 wells, each row of 8 wells is overlaid with 180 µl of media. Embryos were not removed from the incubators during the observation periods, and media was not changed. Each time-lapse video exported had a frame-rate of 5–10 frames an hour. All images were irreversibly anonymized by clinic staff before being given to us.

The dataset comprised fresh ICSI transfers from 2016 to 2019 that resulted in either live birth or no pregnancy (defined as no pregnancy ever detected, including miscarriages and biochemical pregnancies), including both single-embryo transfers (SET) and double-embryo transfers (DET). Only DET that resulted in no pregnancy or male/female twins (to exclude the possibility of monozygotic twinning) were included. In total, we used time-lapse videos for 443 successful embryos and 257 unsuccessful embryos.

### Preparation of input image data

The frame numbers of specific stages in development were recorded by viewing each video in ImageJ. The frames at various time intervals before and after this moment were then automatically extracted using the timestamp (displayed in the bottom right of each frame). Measuring time in hours rather than frames was necessary as the time between frames was inconsistent between videos.

The datasets for each stage contained a frame from almost every embryo in the whole time-lapse dataset of 700 videos; however, there were a small number of frames where the image quality was too low or the specific moment could not be determined (due to out-of-focus cell divisions or excessive

fragmentation), therefore 10 embryos were excluded from the PN dataset, 13 from the 4-cell dataset, and 15 from the 8- to 16-cell dataset. We ensured that the Embryoscope™/Embryoscope+™ ratio was equal across the two groups by randomly removing some of the successful Embryoscope embryos (this group initially had more embryos recorded by the Embryoscope).

All images before the blastocyst stage were cropped to 300 × 300 pixels as this was the smallest size that captured the whole embryo including the zona. As embryos at the blastocyst stage expand a variable amount, occasionally almost filling the image, this stage was left uncropped. All images were then resized to 224 × 224 as this is the input size required by the pre-trained model.

### Model

The model we have used is the MobilenetV2 model [24], a CNN for which weights pre-trained on the ImageNet [25] database are available. Using these weights allowed us to easily implement transfer learning from ImageNet, a standard strategy for relatively small datasets that is often used in studies classifying human embryos [8, 10, 11, 13, 14, 17–19, 22, 26]. MobileNetV2 is one of the commonly used models in computer vision and has previously been shown to be capable of successfully classifying medical images by several studies [27–30]. In addition, MobileNetV2 is a computationally light model, therefore is convenient for any clinics wishing to repeat model training on their own dataset. We used fixed convolutional features, training only the final layer of the model. Prior to hyper-parameter tuning, we used a base learning rate of 0.0001, a dropout of 0.5, and the cross-entropy loss function. For the live birth prediction models, we applied a class weight of 2 to the live birth class to account for this class having about half the amount of data as the no pregnancy class.

For the live birth prediction models, we also experimented with using developmental stage classification for extra domain-specific transfer learning. The first step was to add an extra hidden layer to the MobileNetV2 model and train it to predict developmental stage with both the hidden layer and last layer trainable (the rest of the network was fixed as before). For stages earlier than the blastocyst, we used the classes as in Fig. 1E for step 1. For the blastocyst stage, we trained a separate model with the before nuclear envelope breakdown (NEBD) class replaced with a blastocyst class. In the second step of training, we then took this model as a starting point for our live birth prediction models, where for this step the only trainable layer was the last layer, while all the convolutional and the hidden layers were fixed. We repeated these two steps with various numbers of hidden units (100, 320, 640, or 960) in the hidden layer to find the most suitable model structure.

### Model training

Two training strategies were used in this work; cross validation, where train/validation/test sets were assigned randomly at the start of each repeat training run, and hold out test set, where training and validation sets were randomly assigned for each repeat run while the test set remained constant. We used an 80:10:10 train/validation/test split for the former and 60:20:20 train/validation/test split for the latter. When assigning embryos to the test and validation sets, we kept embryos from the same cycle together for the live birth prediction models to avoid data leakage. We also kept the proportion of SET to DET constant throughout the train/validation/test sets. We then performed augmentation on the training set by rotating each image by 90, 180, and 270 degrees and getting the mirror image.

Each training attempt was repeated twice, the first time we ran each model for 10 000 epochs and recorded at what epoch the validation set peaked in performance on average across all repeat training runs. The second time we trained the model for this optimal number of epochs for every repeat training run. We did this because our models were prone to overfitting, so finding the optimal number of epochs was important; however, the small size of our validation set led to a lot of fluctuation, so averaging over many repeat runs was required.

### Model performance evaluation

For each model setup, we ran 50 repeat training runs and for each training run the area under the curve (AUC) of the receiver operator characteristic (ROC) was calculated. The ROC is a graphical plot of true-positive rate versus false-positive rate at various thresholds. The AUC of this curve is therefore a measure of how well the model performs, with a value of 1 corresponding to a perfect classifier. We calculate the ROC AUC using Scikit-learn python library. The standard error in ROC AUC values over all repeat runs was then used to calculate error bar values.

The blastocyst model was compared to the embryologist scoring system using grades assigned by the embryologists at St Mary's. An overall 'embryologist score' was calculated from averaging TE, ICM, and expansion scores; while we acknowledge that this scoring system is imperfect, as in reality, the embryologist selecting the embryo may be able to select the better embryo out of embryos given the same grade and may place a different level of importance on the individual expansion/TE/ICM scores. However, due to the lack of an evidence base for selecting amongst embryos of similar grades, we decided that a simple average would be best for calculating an overall score, allowing for a comparison with our blastocyst model.

The comparison of model performance at the optimal time-point versus the time-point 6 h before (Fig. 3) was carried out by a Student's t-test. The significance between the success rates of subsets of the high-quality blastocysts (HQB) group and the whole HQB group (Fig. 4B) was calculated using a binomial test.

## Results

In this study, we employed CNNs to analyse the biological process of human pre-implantation development and provide information of clinical relevance. To this end, we trained and tested CNN models on a dataset of time-lapse videos of embryos (700 in total) with known transfer outcomes from the IVF clinic at the Department of Reproductive Medicine, St Mary's Hospital, Manchester, UK. This is an NHS-funded clinic with stable patient population demographics and standardized treatment policies, and therefore highly suitable for single-centre treatment outcome studies [31]. Embryos were cultured in either Embryoscope<sup>TM</sup> or Embryoscope+<sup>TM</sup> time-lapse incubator system (Vitrolife, Sweden).

Live birth prediction is a difficult task as some embryos fail due to maternal factors rather than defects of the embryo itself. This essentially adds 'label noise' to the data; some 'unsuccessful' embryos will actually be of a high quality and likely developmentally competent. This means that there is an upper limit to the live birth prediction success rate as it is impossible to be certain or close to certain that a high-quality embryo will be successful. Therefore, in addition to predicting live birth, we first trained and tested models on the simpler task of developmental stage classification in order to fully evaluate the capabilities of our ML framework on this dataset.

### Developmental stage classification

To develop stage classification models, all time-lapse videos had one frame manually extracted for each developmental stage, resulting in equal class sizes. To reduce the amount of training data needed, we used the established practice of transfer learning, using the MobileNetV2 model with layers pre-trained on ImageNet, a large dataset of various images commonly for pre-training when classifying human embryos [8, 10, 11, 13, 14, 17–19, 22, 26]. The overall workflow is illustrated in Fig. 1B.

First, we trained a binary model to classify embryos as zygote or two-cell stage (Fig. 1C). Subsequently, we trained a second binary model to recognize subtler differences on the subcellular level. To this end, we used images of embryos taken before or after NEBD (Fig. 1D). The two investigated models were trained with varying amounts of training data by randomly excluding a portion of our dataset. The training set size ranged from 10 to 1200 (all data used—600 embryos remain after some are assigned to test/validation sets and 2 images are taken from each embryo) with and without data augmentation. The validation and test sets were kept constant at 100 images each. The average test set scores (Fig. 1C and D) showed that when all the data were used, we reached a test set accuracy of 97.1% for the zygote versus two-cell model and 94.6% for the before NEBD versus after NEBD model.

For both models, the accuracy increased with the amount of training data, as expected, and appeared to be reaching a plateau in performance once the number of images in the training set rose to around 200–400. This plateau may suggest that the model performed close to its optimal level and we are not likely to gain much better performance by adding more training data. Visual inspection of the images (Supplementary Fig. s1A) also suggested that there is an upper limit to the accuracy that could be obtained as vacuoles, and cells dividing in a plane that does not allow subsequent blastomeres to be immediately identified can cause an embryo to appear to be at a different stage when viewed without the context of the time-lapse video.

Our results also confirmed that relatively high performances can be achieved even with very little data. Over 85% test set accuracy was obtained for both models with a training set size of just 10 (five images from each stage). This performance can be partly attributed to the fact that the classification task here is very straightforward with a clear morphological difference between the classes and very little label noise; however, it is also likely to be due to the pre-training on ImageNet resulting in pre-trained features that are transferable to this setting. Figure 1C and D also shows that augmentation (see Materials and methods section for details) seemed to have a small but positive effect, especially with limited training data, so we chose to continue using augmentation going forward.

We then trained multi-class models to classify images into five output classes corresponding to the consecutive stages of human pre-implantation development (Fig. 1E). We saw that a test set accuracy of 87.7% was achieved, which is much higher than the by-chance score of 20%. The results in Fig. 1E show a similar trend to the one observed in the binary models, where increases in accuracy became small once the training set reached about 200–400 images, and a reasonably high test set accuracy (69.4%) was achieved even with a training set of just 10. These results further confirm that MobileNetV2 with pre-trained layers can achieve a high performance, even with a small amount of the training data, when analysing routinely collected images of pre-implantation human embryos.

## Live birth prediction at blastocyst stage

Following the successful creation of developmental stage classifiers, we next used the same model framework (MobileNetV2 with transfer learning via layers pre-trained on ImageNet) to predict live birth based on the blastocyst stage, as this stage is most commonly used for embryo assessment and is a good time-point for comparisons. We extracted the final frame from each time-lapse video to produce a dataset of blastocyst images and trained the model on this dataset using 5-fold cross validation with 50 repeat training runs for each fold. For each embryo in the dataset, we calculated an average model confidence score from all 50 training runs where that embryo was in the test set. We then calculated the ROC AUC; the AUC (called the ROC curve) that is created by plotting true-positive rate versus false-positive rate at various thresholds. A ROC AUC of 0.5 is no better than chance and 1 is a perfect model, we achieved a ROC AUC of 0.680 for live birth prediction at blastocyst stage.

Next, we wished to compare our results against embryologist selection performance. To do this, we used a subset of embryos (141 in total) for which Gardner grades [32] (a set of ICM, TE, and expansion scores standardly used by embryologists when assessing blastocysts) were available to produce ROC curves using the average model confidence scores and embryologist grades. In order to produce the ROC curve from embryologist grades, we first converted the Gardner score letter grades into numbers, as proposed by Alpha Scientists in Reproductive Medicine and ESHRE Special Interest Group of Embryology [33]. Then an overall score was obtained by calculating an average of TE, ICM, and expansion scores.

The ROC curves for both blastocyst assessment methods are shown in Fig. 2A. The ROC AUC was similar for embryologist and model assessment at 0.720 and 0.726, respectively. This suggests our model had a very similar performance to highly trained embryologist grading, as St Mary's Clinic hosts the UK National External Quality Assessment Service (a charitable consortium of external quality assessment laboratories) in reproductive biology. It is, however, important to note that the ML blastocyst model was at a disadvantage due to the use of limited information; only a single focal plane from just the final frame was used to train the ML model. In contrast, the assessment of the embryologist was done using multiple focal points from the final frame, with possible adjustment of the score according to the time-kinetic data.

In clinical practice, a numerical scoring system of embryo viability is more useful than a binary 'successful' or 'unsuccessful' prediction, as it allows the embryos in a cohort to be ranked in order of likelihood of live birth. Although our model was trained as a binary classifier, the confidence score is continuous. Confidence calibration varies between modelling systems [34], therefore it was necessary to determine whether our model confidence scores could be useful in ranking embryos. To investigate this, we sorted all the embryos in our dataset into buckets by average test set model score, with bucket 1 being the lowest score and bucket 10 being the highest score. The success rate (number of successful embryos in bucket/total number of embryos in bucket) for each bucket is shown in Fig. 2B. There was a general increase in success rate from buckets 1 to 10, suggesting that the confidence score was correlated to chance of live birth and therefore could be useful as a method to rank embryos in a cohort. However, the increase in success rate with bucket number appeared to plateau from buckets 7 to 10, suggesting that there is a subset of HQB for which any further increase in model score has little correlation to increased chance of live birth. Analysing embryologist grade versus live birth for a dataset of fresh

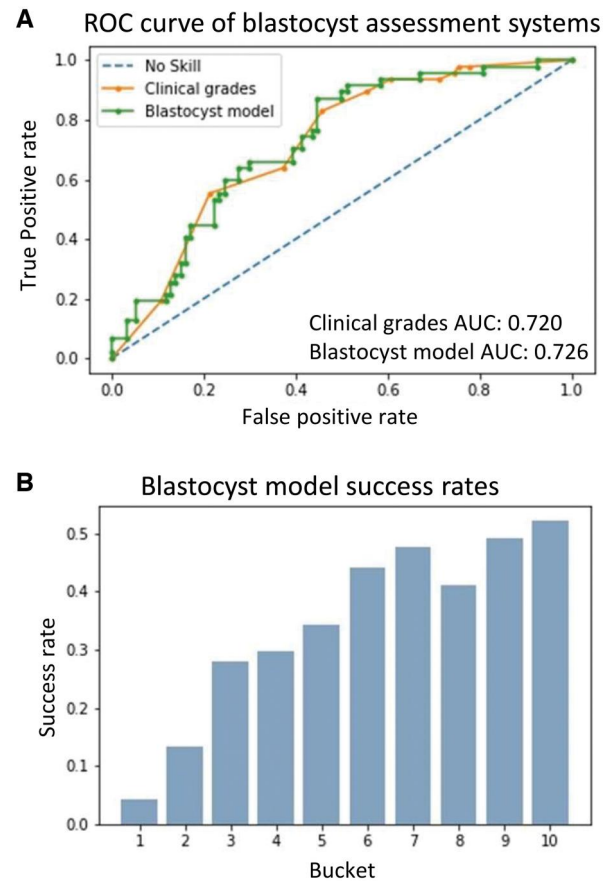


**Figure 2.** Live birth predicted from blastocyst stage. The blastocyst model predicts live birth using the last frame of the time-lapse video on day 5, the predictions produced by this model are a number between 0 and 1, 0 corresponding to an unsuccessful transfer (no pregnancy) and 1 corresponding to a successful transfer (resulting in live birth). The model scores used here are an average over 50 models (using 5-fold cross-validation and 50 training attempts for each fold). (A) A comparison between the performance of average model score and embryologist grading. Only embryos for which clinical grades were available were included, a total of 141. The clinical grades were originally based on the Gardner scoring system, and were then converted into numerical grades to allow a ROC curve to be generated. (B) The correlation between live birth success rate and average model score, using cross-validation test scores for the whole dataset (700 embryos). The embryos have been sorted into buckets from 1 to 10 based on average model score, bucket 1 is the lowest scoring embryos and bucket 10 is the highest scoring embryos. The success rate of each bucket is the fraction of embryos in the bucket that resulted in a live birth.

blastocyst transfers from St Mary's, we observed a similar plateau (Supplementary Fig. S2A), suggesting that this is an issue for both ML and embryologist-based approaches.

Our data demonstrated that it is possible to train MobileNetV2 to predict live birth from blastocyst morphology to a performance similar to embryologist assessment, with the potential for further improvements to performance. Importantly, using both the ML and embryologist scores, we have identified a limitation to embryo assessment based on blastocyst images; above a certain quality threshold, it appears to be difficult to discriminate further the most viable embryo from a group.

## Identification of developmental time-points most indicative of viability

Currently, embryo assessment is based predominantly on the morphology of the embryo at the blastocyst stage. To establish

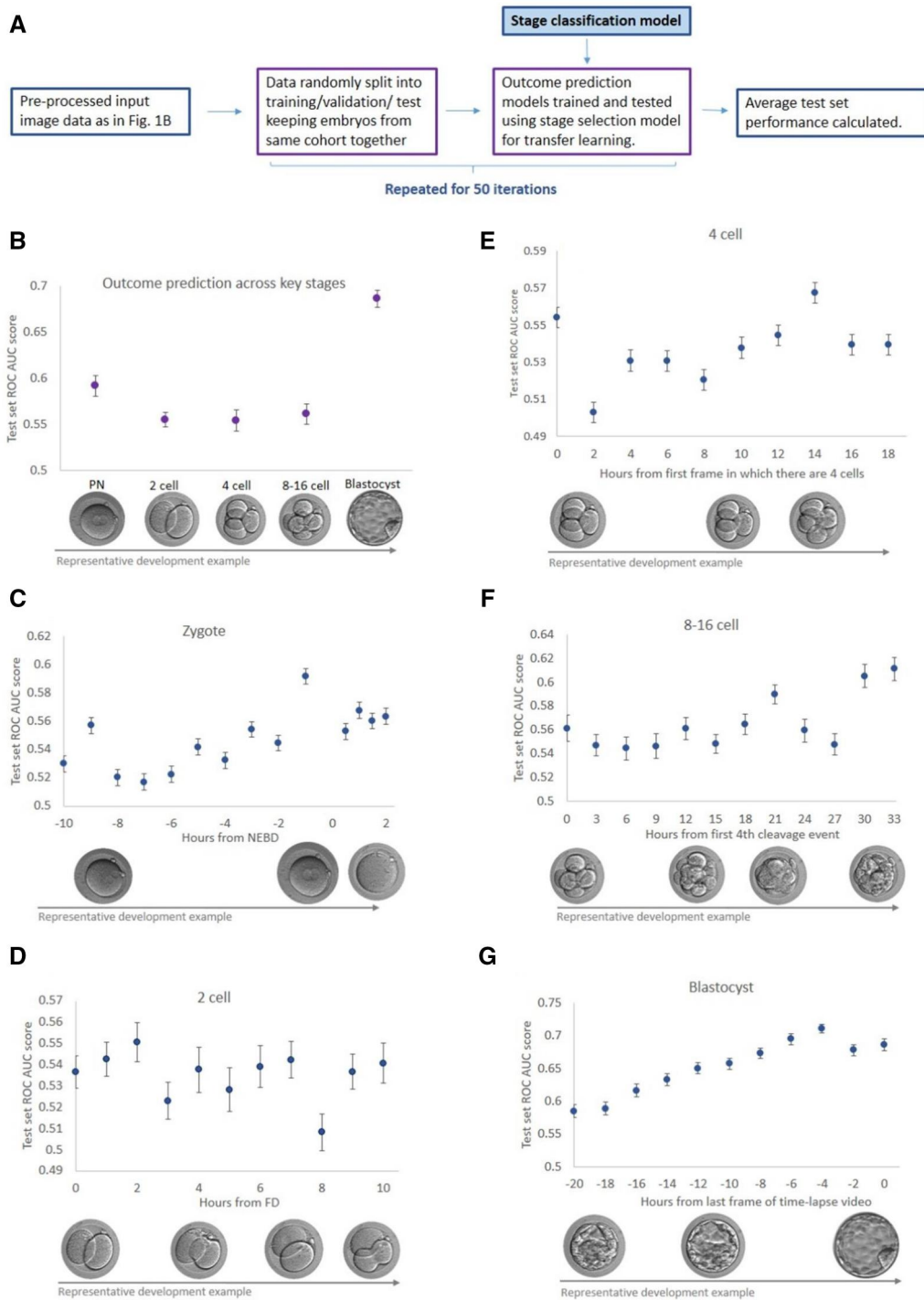


**Figure 3.** Predicting Live birth from a transferred embryo using specific time-points across development. All ROC AUC scores shown here are the average ROC AUC scores on the test set after 50 training iterations each with a different randomly allocated train/validation/test split with 25 embryos in the successful class and 48 embryos in the unsuccessful class for both the test and validation set. The accompanying error bars are the standard error across these 50 training attempts. **(A)** The methodology for developing the live birth prediction models. **(B)** The ROC AUC scores for models trained to predict live birth using images from precisely defined moments of development. ‘PN’ is 1 h before completion of NEBD, ‘2 cell’ is first frame with 2 cells, ‘4 cell’ is first frame with 4 cells, ‘8–16’ cell is the first fourth cleavage event, and ‘blastocyst’ is the last frame of the video. **(C)** The ROC AUC scores for models trained to predict live birth using images at various time intervals before and after NEBD. **(D)** The ROC AUC scores for models trained to predict live birth using images at various time intervals after first division (FD). **(E)** The ROC AUC scores for models trained to predict live birth using images at various time intervals after the first frame with 4 cells. **(F)** The ROC AUC scores of the test set for models trained to predict live birth using images at various time intervals after the first fourth cleavage event. **(G)** The ROC AUC scores for models trained to predict transfer live birth using images at various time intervals before the last frame of the time-lapse video.

whether earlier stages can also be useful in assessing embryo viability, we extracted frames from each time-lapse video in the dataset at four pre-blastocyst stages that could be precisely

defined; 1 h before NEBD completion, the first appearance of 2 cells, first appearance of 4 cells, and initiation of 8- to 16-cell division round, we referred to these stages as pronuclear (PN), 2-cell,

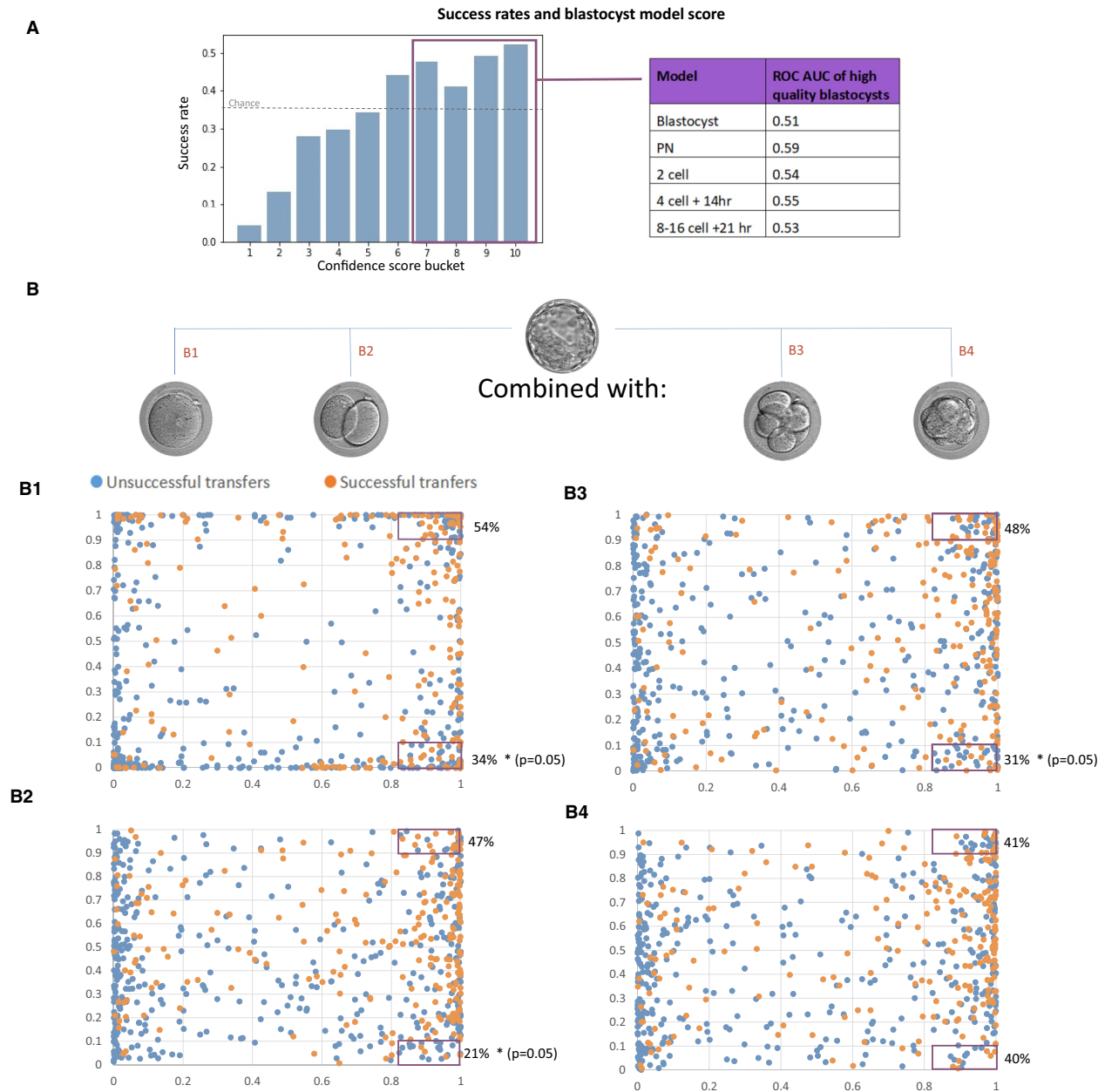


**Figure 4.** Ranking embryos by blastocyst model score and combining model outputs. **(A)** The association between live birth success rate and blastocyst model prediction (a model trained to predict live birth from images taken at blastocyst stage). The embryos have been sorted into buckets by blastocyst model confidence score, bucket 1 is lowest and bucket 10 is highest. The figure (left) shows the success rate of each bucket, defined as the fraction of embryos in each bucket that resulted in a live birth. The table on the right shows the ROC AUC for embryos in buckets 7–10 (‘high quality blastocysts’—259 in total) obtained using each of the models trained in this study. **(B)** B1–4 blastocyst model score versus PN, 2-cell, 4-cell +14 h, and 8- to 16-cell +21 h model score, respectively. The probability of live birth for HQB (see A above) with a very high pre-blastocyst model score ( $>0.9$ ) or very low pre-blastocyst model score ( $<0.1$ ) is also shown for each figure.

4-cell, and 8- to 16-cell, respectively. Subsequently, live birth prediction models were trained using each stage (following the workflow illustrated in Fig. 3A).

As predicting live birth from embryo morphology alone is a difficult task, we decided to use our multi-class stage classification model as an extra domain-specific transfer learning step (see Materials and methods section for full details). We experimented with various hyper-parameters, and the results for all stages are shown in Supplementary Fig. S3A. Our results suggest that this domain-specific transfer learning step generally improved model performance, particularly for the PN and 4-cell models.

The ROC AUC values reported in Supplementary Fig. S3A were the average of 50 repeat training runs each with a different randomly selected test set, as we had observed that variation due to the training uncertainty was minor compared to variation due to changes in the test set. This also allowed for a quicker investigation than the 5-fold cross-validation with 50 training attempts used in the previous section. We chose to use varying test sets to increase statistical power as we found that separate test sets had a higher than desirable variability in performance, reflecting the heterogeneity of the data in this ML task (Supplementary Fig. S3B). However, the transfer model was trained on the same data-set, so to check this was not resulting in an unfair bias, it was

**Table 1.** Performance on a hold out test using either the original MobileNetV2 model with fixed features up to the last layer or the MobileNetV2 model with fixed features and extra transfer learning; an extra hidden layer before the last layer has been pre-trained as a stage classifier

Stage	ROC AUC when standard MobileNetV2 model used, 95% CI	ROC AUC when extra transfer learning used, 95% CI
PN	0.547 (0.540–0.553)	0.557 (0.553–0.562)
2-cell	0.555 (0.546–0.564)	0.520 (0.511–0.528)
4-cell	0.533 (0.524–0.541)	0.578 (0.570–0.586)
8- to 16-cell	0.578 (0.570–0.586)	N/A
Blastocyst	0.714 (0.710–0.718)	0.703 (0.700–0.706)

The number of hidden units in the last layer is the amount we found to be optimal for that developmental stage. ROC AUC scores shown here are the average scores on the test set over 50 training iterations. The 95% CI has been calculated from the standard error across these 50 training attempts. The test set contained 50 embryos in the successful class and 96 embryos in the unsuccessful class. N/A=Not Applicable.

necessary to also develop all models from scratch with a true ‘hold out test set’—a test set separated out at the very start, prior to training the transfer model. As shown in Table 1, our results continue to hold up in this control experiment, the PN and 4-cell stage do significantly better with extra domain-specific transfer learning ( $P < 0.05$  and  $P < 0.001$ , respectively), so going forward, we used extra domain-specific transfer learning (with our optimized hyper-parameters) for the PN and 4-cell models in addition to the transfer learning from ImageNet (via the pre-trained layers) used for all other stages.

The average test set ROC AUC (and accompanying standard errors as error bars) over 50 training attempts with random train/validation/test split is shown in Fig. 3B for each stage. The blastocyst stage has the most obvious morphological differences between classes, with unsuccessful embryos less likely to form expanded blastocysts, and as expected, this model had the best performance. The low ROC AUC reported for pre-blastocyst stages is unsurprising due to the difficulty of this prediction task, as reflected by the lack of studies reporting highly successful live birth prediction using pre-blastocyst stages. In addition to confounding maternal factors, at early stages, there is the added challenge that the majority of developmentally abnormal embryos are not yet identifiable by morphology. Despite these issues, the pre-blastocyst models still gave above chance predictions. From these results, it was clear that different developmental stages carry different predictive power. To identify specific moments in development for which live birth predictions are the most successful, we tested multiple time-points at regular intervals using each of the previous developmental stages as reference points (Fig. 3C–G).

We found that the model performance varied at different time-points and appeared to peak at certain moments in development as shown in Fig. 3C–G. For the PN stage (Fig. 3C), a performance peak was observed just before NEBD. Performance across the 2-cell stage (Fig. 3D) was variable with no peak seen. A performance peak was observed 14 h after 4-cell (Fig. 3E), this generally is within the 4- to 8-cell transition; however, no potential explanation for this peak was found from visually examining the time-lapse videos. Another performance peak was observed 21 h after initiation of the 8- to 16-cell cycle (Fig. 3F) when embryos tend to be in the morula stage. As an initial examination of the time-lapse videos suggested that this was generally just before cavitation, we then quantified this by counting the number of cavitating embryos at this time-point and at time-points just before and after. The results, shown in Table 2, confirmed that this performance peak corresponds to the moment just before cavitation. Lastly, the blastocyst stage showed a gradual improvement in model performance towards the end of the time-lapse video

**Table 2.** Percent of embryos that have begun cavitating in each group at various time-points after first fourth cleavage event

Hour	Percent of embryos cavitating	
	Successful (%)	Unsuccessful (%)
21	7.3	4.8
24	27.4	21.9
27	50.9	40.0
30	81.2	50.8

(Fig. 3G), appearing to reach a plateau 6 h before the last frame, by which point the successful embryos have usually formed an expanded blastocyst. We found that the peaks at PN, 4-cell +14 h and 8- to 16-cell +21 h were all statistically significant when compared to a time-point 6 h earlier ( $P$ -values of 0.0001, 0.0005, and 0.0011, respectively), determined by a Student's  $t$ -test on scores from the 50 training attempts at each time-point.

Finally, to test the potential benefit of averaging over repeat training attempts and also to obtain a single prediction for each embryo in our dataset (to be used in further investigations reported below), we re-trained each model using 5-fold cross-validation with 50 repeat training runs to calculate an average test set model score for each embryo as in the previous section. The PN, 2-cell, and blastocyst stage models were trained using the original time-point and the 4-cell and the 8- to 16-cell stage models were trained using the peak performance time-point (4-cell +14 h and 8- to 16-cell +21 h). The ROC AUC scores calculated from these average model scores (Table 3) showed that slightly better predictions can be made when the model score assigned to an embryo is averaged over many separately trained models, which is consistent with the existing literature on ensemble learning [35]. Additionally, we then also used the embryo average scores to calculate F1 and precision-recall AUC for each model (Supplementary Table S1) for further validation.

### Combined model outputs allow refined ranking of high-grade blastocysts

We next wanted to investigate whether information from the identified developmental time-points could provide insight into the HQB group identified previously and assist in embryo selection. To test this, we calculated the ROC AUC of models at each stage on just the HQB group. The results (Fig. 4A) show that the blastocyst model performed almost no better than chance and worse than all the earlier-stage models, and the PN model performed the best. This suggests that if multiple embryos in a cohort fall into this HQB group (blastocyst model score  $> 0.83$ ), then pre-blastocyst stage models should be used to choose which one



**Table 3.** Effect of averaging score from many models rather than using just one model

Stage	Average Individual ROC AUC	ROC AUC using average confidence score
PN	0.591 ± 0.0115	0.603
2-cell	0.555 ± 0.00779	0.575
4-cell	0.567 ± 0.0114	0.581
8- to 16-cell	0.585 ± 0.00779	0.585
Blastocyst	0.686 ± 0.00937	0.680

The average individual ROC AUC scores are the average scores on the test set after 50 training iterations each with a different randomly allocated train/validation/test split with 25 embryos in the successful class and 48 embryos in the unsuccessful class for both the test and validation set. The accompanying errors are the standard error across these 50 training attempts. For the ROC AUC using average confidence score, the average confidence score was first calculated from 50 models (using 5-fold cross-validation and 50 training attempts) and these average confidence scores were then used to calculate the ROC AUC.

of these HQB embryos to transfer, rather than simply choosing the one with the highest blastocyst score.

To further investigate the benefit of using earlier-stage models in conjunction with the blastocyst model, we plotted the pre-blastocyst score versus blastocyst score for each embryo, as shown in Fig. 4B. These figures provide a visualization of the spread of scores assigned by each model and the correlation between earlier-stage scores and blastocyst score. We noticed that the model confidence scores had a tendency to be close to the extreme values; 0 or 1. To further investigate the added value of the pre-blastocyst stage models, we calculated the success rate of the HQB embryos when the pre-blastocyst model score was >0.9 versus <0.1. This was then compared with the success rate of the HQB group as a whole (0.47) to calculate significance. We found that the success rate was significantly lower ( $P=0.05$ ) when the PN, 2-cell, or 4-cell +14 h model score is <0.1. This suggests that the early models are most useful at identifying low-quality embryos in the HQB group. This adds further evidence that there are developmentally abnormal embryos in the HQB group and pre-blastocyst model predictions should be taken into account when selecting from this group.

## Discussion

A better understanding of the processes driving human pre-implantation development can help with embryo selection for IVF and assure that the best-quality embryos are chosen for the transfer. Here, we identified previously unreported windows of development that are most closely linked to embryo viability and demonstrated that predictions from these developmental stages can be used to refine the selection for transfer of high-quality blastocysts. Embryo assessment, both manual and ML, typically has an emphasis on specifically chosen time-points; however, these may not necessarily be the optimal moments of embryo development for assessing viability. We found the performance of live birth predictor models varied considerably depending on the exact moment in development in which they were trained, with peaks in performance found at multiple developmental stages. This could possibly be part of the reason for disagreements in the findings of studies linking embryo morphology to viability (e.g. the effect of vacuoles at the zygote stage [36, 37], as it is possible that researchers do not always use the exact same moments in development. Our findings could inform future embryo viability studies, as we have provided guidance on which developmental time-points to focus on. This could be particularly valuable for

the morula, as there has been limited research into this stage, yet our research suggests that during a specific window, it may contain important information about embryo viability. Additionally, the plateau in performance found at the blastocyst stage suggests the possibility that longer culture of the blastocyst beyond this point might not result in increased accuracy in assessment, highlighting an interesting avenue for further investigation.

We noticed that the peaks in model performance found at the PN stage and 8- to 16-cell +21 h are both just before certain well-described developmental events: NEBD and blastocyst cavitation, respectively. There are two possible explanations for this: at these pre-event time-points, there is less natural variation in the appearance of viable embryos (compared to time-points where the embryo is undergoing processes such as PN growth or compaction) so it is easier to distinguish important developmental abnormalities, or these may be biologically important moments where any deviation from normal development can prevent the embryo from developing properly. For example, the ability of embryos to correctly prepare and execute the first mitosis is one of the defining moments of development and any anomalies around this time, such as problems with the NEBD process, can result in developmental failure. The peak during the transition from the 4- to 8-cell stage coincides with embryonic genome activation in human embryos [38, 39], raising the possibility that there are some morphological manifestations that can indicate the successful activation of the genome.

Finally, we investigated whether the previously identified key moments of development could help to understand the nature of the HQB group—a sub-group of embryos that all had a blastocyst model score above a certain threshold where any further increase in model score seemed to be unrelated to further increase in viability. It was not clear whether all the embryos in this group were of high quality and just failing for non-embryonic (e.g. uterine) reasons, or if there were embryos within the group that had developed abnormally despite receiving a high blastocyst model score. Our findings suggested the latter is true, as we found that it was possible to use the pre-blastocyst models to identify HQB embryos that were less likely to result in live birth. This provides evidence that predictions from early development may be used in conjunction with predictions from the blastocyst stage to give a better assessment of embryo quality than the blastocyst model alone. In addition to embryo selection, it is also possible that the pre-blastocyst models could be used to help diagnose the reason for IVF transfer failure, if all HQB blastocysts in cohort fail to result in live birth, then the earlier model predictions could provide an indication of whether there were embryonic issues not detectable at blastocyst stage or if the issue is more likely to be related to the uterus.

Additionally, our findings could be used to support earlier transfers. Extending the culture until the blastocyst stage is associated in some studies with a number of adverse outcomes, such as pre-term birth, altered birthweight, mono-zygotic twinning, and shortened telomeres [40–44]. These disadvantages are not unexpected, since blastocyst culture acts to expose embryos to selection stress in a non-physiological in vitro environment, at the precise time in development when the embryonic genome and epigenome are being reset as part of the formation of a new individual [44–46]. Blastocyst culture is currently favoured as it leads to significantly higher live birth rate per transfer and per embryo [47]; however, the cumulative live birth rate, including transfer of all fresh and frozen embryos from a single egg collection event, is not necessarily increased using this policy. Our findings provide the flexibility of making viability assessments at

various points in development, supporting various clinical strategies.

One of the biggest common limitations to ML is large data requirements. However, the models trained here demonstrate the potential of carrying out a CNN-based analysis of a biological process without needing large amounts of training data. Our blastocyst model was competitive with highly trained embryologists and obtained a similar performance to other studies that used CNNs to predict live birth [20–22], despite being trained on a single-clinic dataset. This suggests that our algorithms could be easily re-trained on an individual clinic's patient population to become specifically tailored to that clinic, which is an important factor as most clinics have distinct treatment policies and patient populations [48]. The high performance achieved in stage classification also demonstrates the high capability of our chosen model on this limited dataset, even for quite subtle subcellular differences such as classifying embryos as before NEBD versus after NEBD. Our stage classification models showed that increases in performance became small when the training set size was increased beyond around 200–400, suggesting that the data amount was not likely to be the main limiting factor in performance.

There are a few limitations to this study which need to be acknowledged. One limitation is that only transferred embryos could be included; ideally, the models would be trained on all embryos in the cohort. However, this is not possible, as a ground truth label can only be assigned to transferred embryos. It would only be possible to determine whether a model could improve live birth rates by conducting a prospective randomized controlled trial. Another limitation is that the comparison between the blastocyst model and embryologist scores slightly underestimates the embryologist's performance, as in reality, the embryologist would use their professional knowledge to differentiate between embryos of the same grade. Additionally, another limitation is that as only one clinic dataset was used in this study, we cannot yet be sure that our findings of the most informative moments in development are universal, it will be necessary to repeat our investigation on datasets from other clinics to verify this. We also only included embryos that resulted in live birth or no pregnancy. Exploring the relevance of our model to miscarriage is an interesting area for future research which would require a larger dataset.

The aim of this study was to provide a better understanding of pre-implantation development in the context of embryo assessment; therefore, we focused on investigating the utility of various developmental stages rather than developing a new state-of-the-art algorithm. With the constant development of different models, it is quite possible that different or more advanced ML techniques could lead to improvements in performance, a comparison of different models would be necessary to get the best possible predictions of live birth. We hope the information provided here can inform future studies on embryo assessment via deep learning and contribute to improving embryo selection procedures before IVF.

There are many areas of further work leading on from this study. For example, further investigation is required to refine the value of the blastocyst model score threshold at which earlier models should be consulted, as an exact threshold would be necessary for clinical decision making. It would also be interesting to try to combine model scores from all stages to try to get an overall improved performance. Previous studies have used multiple stages simultaneously [12, 15, 17, 22, 23], and in some cases have found this can improve performance [11], likely due to the

inclusion of temporal information about how the embryo develops over time, as well as providing more information to guide the model overall. As far as we are aware, no studies include all frames, but rather extract frames at given intervals, possibly due to computational restraints or concerns about overfitting. Therefore, it would be interesting to see if an improvement could be found if our findings were used to guide frame selection and ensure the most informative moments were included. Additionally, it could also be interesting to see if better overall predictions could be obtained from a model combining embryologist grades and CNN model scores.

## Conclusion

In summary, we have identified specific windows of early development that are most predictive of live birth by applying a readily accessible, pre-trained CNN (MobileNetV2) to hospital-specific image data. We have also provided evidence that information from the identified developmental time-points most indicative of viability could be combined with blastocyst stage model predictions to give better overall embryo assessment than selecting based solely on blastocyst morphology. Finally, the application to a single-clinic dataset, of limited size, highlights the feasibility of exploiting state-of-the-art ML techniques in individual clinic settings, while being able to capture and cater for local protocols and data heterogeneity.

## Acknowledgements

We would like to thank other members (current and past) of the Plusa lab for their discussion about the article.

## Author contributions

Camilla Alice Mapstone (Data curation [equal], Formal analysis [lead], Funding acquisition [supporting], Investigation [lead], Methodology [equal], Software [lead], Writing—original draft [lead], Writing—review & editing [equal]), Helen Hunter (Data curation [lead], Formal analysis [supporting], Writing—review & editing [equal]), Daniel Brison (Conceptualization [equal], Data curation [equal], Writing—review & editing [equal]), Julia Handl (Formal analysis [supporting], Funding acquisition [supporting], Methodology [equal], Supervision [equal], Writing—review & editing [equal]), and Berenika Plusa (Conceptualization [equal], Funding acquisition [equal], Project administration [lead], Supervision [lead], Writing—review & editing [equal])

## Supplementary data

[Supplementary data](#) is available at *Biology Methods and Protocols* online.

*Conflict of interest statement.* The authors declare no competing interests.

## Funding

C.M. was sponsored by the Wellcome Trust as part of the Quantitative and Biophysical Biology programme (220001/Z/19/Z). Funding to B.P Lab was provided by the Wellcome Trust grant Seed Awards in Science (212372/Z/18/Z). D.B was funded by Manchester University NHS Foundation Trust.

## Data availability

The data that support the findings of this study are available from the corresponding author upon reasonable request. The code used to build the models is available at <https://github.com/CMapstone/eMLife>.

## Ethics

As this research used only fully anonymized, routinely collected data, ethical approval was not required in accordance with the NHS Health Research Authority (HRA) guidelines (<http://www.hra-decisiontools.org.uk/ethics/>). Therefore, written consent from participants was waived.

## References

- Bhardwaj A, Kishore S, Pandey DK. Artificial intelligence in biological sciences. *Life (Basel, Switzerland)* 2022;**12**:1430. <https://doi.org/10.3390/life12091430>
- Bhosale YH, Patnaik KS. Application of Deep Learning Techniques in Diagnosis of Covid-19 (Coronavirus): A Systematic Review. *Neural Process Lett* 55, 3551–603. 023. <https://doi.org/10.1007/s11063-022-11023-0>
- Anwar SM, Majid M, Qayyum A et al. Medical image analysis using convolutional neural networks: a review. *J Med Syst* 2018;**42**: 226–13. <https://doi.org/10.1007/s10916-018-1088-1>
- Kushnir VA, Smith GD, Adashi EY. The future of IVF: the new normal in human reproduction. *Reprod Sci* 2022;**29**:849–56. <https://doi.org/10.1007/s43032-021-00829-3>
- Apter S, Ebner T, Freour T et al.; ESHRE Working group on Time-lapse Technology. Good practice recommendations for the use of time-lapse technology. *Hum Reprod Open* 2020;**2020**:hoaa008. <https://doi.org/10.1093/hropen/hoaa008>
- Cimadomo D, Sosa Fernandez L, Soscia D et al. Inter-centre reliability in embryo grading across several IVF clinics is limited: implications for embryo selection. *Reprod Biomed Online* 2022;**44**: 39–48. <https://doi.org/10.1016/j.rbmo.2021.09.0221472>
- Phusa B, Piliszek A. Common principles of early mammalian embryo self-organisation. *Development (Cambridge)* 2020;**147**: dev183079. <https://doi.org/10.1242/dev.183079>
- Bormann CL, Thirumalaraju P, Kanakasabapathy MK et al. Consistency and objectivity of automated embryo assessments using deep neural networks. *Fertil Steril* 2020;**113**:781–7.e781. <https://doi.org/10.1016/j.fertnstert.2019.12.004>
- Kragh MF, Karstoft H. Embryo selection with artificial intelligence: how to evaluate and compare methods? *J Assist Reprod Genet* 2021;**38**:1675–89. <https://doi.org/10.1007/s10815-021-02254-6>
- Khosravi P, Kazemi E, Zhan Q et al. Deep learning enables robust assessment and selection of human blastocysts after in vitro fertilization. *NPJ Digit Med* 2019;**2**:21–21. <https://doi.org/10.1038/s41746-019-0096-y>
- Kragh MF, Rimestad J, Berntsen J et al. Automatic grading of human blastocysts from time-lapse imaging. *Comput Biol Med* 2019; **115**:103494. <https://doi.org/10.1016/j.combiomed.2019.103494>
- Tran D, Cooke S, Illingworth PJ et al. Deep learning as a predictive tool for fetal heart pregnancy following time-lapse incubation and blastocyst transfer. *Hum Reprod* 2019;**34**:1011–8. <https://doi.org/10.1093/humrep/dez064>
- Kanakasabapathy MK, Thirumalaraju P, Bormann CL et al. Development and evaluation of inexpensive automated deep learning-based imaging systems for embryology. *Lab Chip* 2019; **19**:4139–45. <https://doi.org/10.1039/c9lc00721k>
- Thirumalaraju P, Kanakasabapathy MK, Bormann CL et al. Evaluation of deep convolutional neural networks in classifying human embryo images based on their morphological quality. *Heliyon* 2021;**7**:e06298. <https://doi.org/10.1016/j.heliyon.2021.e06298>
- Liao Q, Zhang Q, Feng X et al. Development of deep learning algorithms for predicting blastocyst formation and quality by time-lapse monitoring. *Commun Biol* 2021;**4**:415–415. <https://doi.org/10.1038/s42003-021-01937-1>
- Huang B, Zheng S, Ma B et al. Using deep learning to predict the outcome of live birth from more than 10,000 embryo data. *BMC Pregnancy Childbirth* 2022;**22**:36–36. <https://doi.org/10.1186/s12884-021-04373-5>
- Lee C-I, Su Y-R, Chen C-H et al. End-to-end deep learning for recognition of ploidy status using time-lapse videos. *J Assist Reprod Genet* 2021;**38**:1655–63. <https://doi.org/10.1007/s10815-021-02228-8>
- Fitz VW, Kanakasabapathy MK, Thirumalaraju P et al. Should there be an "AI" in TEAM? Embryologists selection of high implantation potential embryos improves with the aid of an artificial intelligence algorithm. *J Assist Reprod Genet* 2021;**38**: 2663–70. <https://doi.org/10.1007/s10815-021-02318-7>
- VerMilyea M, Hall JMM, Diakiw SM et al. Development of an artificial intelligence-based assessment model for prediction of embryo viability using static images captured by optical light microscopy during IVF. *Hum Reprod* 2020;**35**:770–84. <https://doi.org/10.1093/humrep/deaa013>
- Miyagi Y, Habara T, Hirata R et al. Feasibility of predicting live birth by combining conventional embryo evaluation with artificial intelligence applied to a blastocyst image in patients classified by age. *Reprod Med Biol* 2019;**18**:344–56. <https://doi.org/10.1002/rmb2.12284>
- Ueno S, Berntsen J, Ito M et al. Pregnancy prediction performance of an annotation-free embryo scoring system on the basis of deep learning after single vitrified-warmed blastocyst transfer: a single-center large cohort retrospective study. *Fertil Steril* 2021; **116**:1172–80. <https://doi.org/10.1016/j.fertnstert.2021.06.001>
- Sawada Y, Sato T, Nagaya M et al. Evaluation of artificial intelligence using time-lapse images of IVF embryos to predict live birth. *Reprod Biomed Online* 2021;**43**:843–52. <https://doi.org/10.1016/j.rbmo.2021.05.002>
- Theilgaard Lassen J, Fly Kragh M, Rimestad J et al. Development and validation of deep learning based embryo selection across multiple days of transfer. *Sci Rep* 2023;**13**:4235–4235. <https://doi.org/10.1038/s41598-023-31136-3>
- Sandler M, Howard A, Zhu M et al. MobileNetV2: Inverted Residuals and Linear Bottlenecks. In: 2018 IEEE/CVF Conference on Computer Vision and Pattern Recognition, Salt Lake City, UT, USA, 2018, pp. 4510–4520, doi: 10.1109/CVPR.2018.00474
- Deng J, Dong W, Socher R et al. Imagenet: a large-scale hierarchical image database. In: 2009 IEEE Conference on Computer Vision and Pattern Recognition, Miami, FL, USA, 2009, pp. 248–255, doi: 10.1109/CVPR.2009.5206848
- Payá E, Bori L, Colomer A et al. Automatic characterization of human embryos at day 4 post-insemination from time-lapse imaging using supervised contrastive learning and inductive transfer learning techniques. *Comput Methods Programs Biomed* 2022;**221**:106895–106895. <https://doi.org/10.1016/j.cmpb.2022.106895>
- Indraswari R, Rokhana R, Herulambang W. Melanoma image classification based on MobileNetV2 network. *Procedia Comput Sci* 2022;**197**:198–207. <https://doi.org/10.1016/j.procs.2021.12.132>

28. Velu S. An efficient, lightweight MobileNetV2-based fine-tuned model for COVID-19 detection using chest X-ray images. *Math Biosci Eng* 2023;**20**:8400–27. <https://doi.org/10.3934/mbe.2023368>
29. Xu L, Mohammadi M. Brain tumor diagnosis from MRI based on Mobilenetv2 optimized by contracted fox optimization algorithm. *Heliyon* 2024;**10**:e23866. <https://doi.org/10.1016/j.heliyon.2023.e23866>
30. Ogechukwu U, Hanan H, Elochukwu U. An evaluation of lightweight deep learning techniques in medical imaging for high precision COVID-19 diagnostics. *Healthcare Analytics (New York, N.Y)* 2022;**2**:100096. <https://doi.org/10.1016/j.health.2022.100096>
31. Castillo CM, Harper J, Roberts SA, et al. The impact of selected embryo culture conditions on ART treatment cycle outcomes: a UK national study, *Human Reproduction Open*, 2020;**2020**(1): hoz031. <https://doi.org/10.1093/hropen/hoz031>.
32. Gardner DK, Lane M, Stevens J et al. Blastocyst score affects implantation and pregnancy outcome: towards a single blastocyst transfer. *Fertil Steril* 2000;**73**:1155–8. [https://doi.org/10.1016/S0015-0282\(00\)00518-5](https://doi.org/10.1016/S0015-0282(00)00518-5)
33. Alpha Scientists in Reproductive Medicine and ESHRE Special Interest Group Embryology. Istanbul consensus workshop on embryo assessment: proceedings of an expert meeting. *Reprod Biomed Online* 2011;**22**:632–46. <https://doi.org/10.1016/j.rbmo.2011.02.001>
34. Guo C, Pleiss G, Sun Y et al. On Calibration of Modern Neural Networks. In: Proceedings of the 34th International Conference on Machine Learning, Sydney, Australia, PMLR 70 2017. <https://doi.org/10.48550/arxiv.1706.04599>
35. Omer S, Lior R. Ensemble learning: A survey. *WIREs Data Mining Knowl Discov* 2018;**8**:e1249.
36. Barberet J, Bruno C, Valot E et al. Can novel early non-invasive biomarkers of embryo quality be identified with time-lapse imaging to predict live birth? *Hum Reprod* 2019;**34**:1439–49. <https://doi.org/10.1093/humrep/dez085>
37. Ebner T, Moser M, Sommergruber M et al. Occurrence and developmental consequences of vacuoles throughout preimplantation development. *Fertil Steril* 2005;**83**:1635–40. <https://doi.org/10.1016/j.fertnstert.2005.02.009>
38. Braude P, Bolton V, Moore S. Human gene expression first occurs between the four- and eight-cell stages of preimplantation development. *Nature (London)* 1988;**332**:459–61. <https://doi.org/10.1038/332459a0>
39. Dobson AT, Raja R, Abeyta MJ et al. The unique transcriptome through day 3 of human preimplantation development. *Hum Mol Genet* 2004;**13**:1461–70. <https://doi.org/10.1093/hmg/ddh157>
40. Glujovsky D, Blake D, Farquhar C et al. Cleavage stage versus blastocyst stage embryo transfer in assisted reproductive technology. *Cochrane Database Syst Rev* 2012;**7**:CD002118–CD002118. <https://doi.org/10.1002/14651858.CD002118.pub4>
41. Castillo CM, Harper J, Roberts SA et al. The impact of selected embryo culture conditions on ART treatment cycle outcomes: a UK national study. *Hum Reprod Open* 2020;**2020**:hoz031. <https://doi.org/10.1093/hropen/hoz031>
42. Zhu Q, Zhu J, Wang Y et al. Live birth rate and neonatal outcome following cleavage-stage embryo transfer versus blastocyst transfer using the freeze-all strategy. *Reprod Biomed Online* 2019;**38**:892–900. <https://doi.org/10.1016/j.rbmo.2018.12.034>
43. De Vos A, Santos-Ribeiro S, Van Landuyt L et al. Birthweight of singletons born after cleavage-stage or blastocyst transfer in fresh and warming cycles. *Hum Reprod* 2018;**33**:196–201. <https://doi.org/10.1093/humrep/dex361>
44. Wang C, Gu Y, Zhou J et al. Leukocyte telomere length in children born following blastocyst-stage embryo transfer. *Nat Med* 2022;**28**:2646–53. <https://doi.org/10.1038/s41591-022-02108-3>
45. Niakan KK, Han J, Pedersen RA et al. Human pre-implantation embryo development. *Development* 2012;**139**:829–41. <https://doi.org/10.1242/dev.060426>
46. Brison DR. IVF children and healthy aging. *Nat Med* 2022;**28**:2476–7. <https://doi.org/10.1038/s41591-022-02098-2>
47. Glujovsky D, Farquhar C, Quinteiro Retamar AM et al. Cleavage stage versus blastocyst stage embryo transfer in assisted reproductive technology. *Cochrane Database Syst Rev* 2016;**2016**: CD002118–CD002118. <https://doi.org/10.1002/14651858.CD002118.pub5>
48. Deshpande P, Gupta A. Causes and prevalence of factors causing infertility in a public health facility. *J Hum Reprod Sci* 2019;**12**:287–93. [https://doi.org/10.4103/jhrs.JHRS\\_140\\_18](https://doi.org/10.4103/jhrs.JHRS_140_18)